Empirical formulas for direct double ionization by bare ions: $Z = -1$ to 92

R. D. DuBois,[1,*] A. C. F. Santos,[2] and S. T. Manson[3]

[1]*Department of Physics, Missouri University of Science and Technology, Rolla, Missouri 65409, USA*

[2]*Instituto de Física, Universidade Federal do Rio de Janeiro, PO 68528, 21941-972 Rio de Janeiro, Rio de Janeiro, Brazil*

[3]*Department of Physics and Astronomy, Georgia State University, Atlanta, Georgia 30303, USA*

(Received 4 April 2014; revised manuscript received 15 July 2014; published 25 November 2014)

Experimental cross sections and cross-section ratios reported in the literature for direct double ionization of the outer shells of helium, neon, and argon atoms resulting from bare ions ranging from protons to uranium and for antiprotons are analyzed in terms of a first- and second-order interference model originally proposed by McGuire [J. H. McGuire, Phys. Rev. Lett. **49**, 1153 (1982)]. Empirical formulas for the various contributions to double ionization plus information about the phase difference between the first- and second-order mechanisms are extracted from the data. Projectile and target scalings are also extracted. Total cross sections and their ratios determined using these formulas and scalings are shown to be in very good agreement with experimental data for lower-Z projectiles and impact velocities larger than 1 a.u. For very-high-Z projectiles, the amount of double ionization is overestimated, probably due to saturation of probabilities that is not accounted for in scaling formulas.

DOI: 10.1103/PhysRevA.90.052721 PACS number(s): 34.50.Fa, 34.80.Dp

I. INTRODUCTION

Experimental studies have shown that multielectron transitions (where two or more outer-shell electrons are ionized) are major contributors to the total ionization cross section in collisions involving heavy particles. From a dosimetry viewpoint, multiple ionization of the target can be far more important than single ionization. This is because the ionization potentials increase rapidly for multiple-electron removal, which means that the energy deposited when multiple ionization occurs is typically significantly larger than for single-electron removal. In addition, multiple ionization of molecules leads to the production of several charged fragments that undergo Coulomb explosion to produce energetic ions capable of inducing subsequent chemical or biological processes. In projectile ionization, multiple ionization can be beneficial in that it is exploited for accelerating particles to high energies or it can be detrimental in high-energy accelerators or storage rings where it leads to beam losses that cause technical problems such as vacuum degradation, erosion of exposed surfaces, and increased radiation levels.

In contrast to excitation or ionization of a single electron by fast bare ions and electrons where perturbation theories such as the first Born approximation can accurately predict total cross sections, modeling multielectron transitions is much more difficult. Unlike the situation for double photoionization, for direct multiple ionization of outer-shell electrons by charged-particle impact the most common approach is to use an independent-electron model (IEM) where the projectile interacts with each target electron independently. In the independent-electron model, the single- and multiple-ionization cross sections scale as $(Ze/v)^{2n}$, where Z and v are the projectile charge and velocity, e is the electron charge, and n is the number of ionized electrons (see [1,2] and references therein). However, two aspects of the independent-electron model that are inconsistent with experimental data are that (a) it predicts the relative amount of double ionization, i.e., $R_2 = \sigma_2/\sigma_1$, which corresponds to $n = 2$ and 1 in the scaling relationships, to steadily decrease and ultimately become negligible for very large v and (b) the double- to single-ionization ratios should be the same for positive and negative values of Z, i.e., for electron and proton impact, positron and electron impact, and antiproton and proton impact. In contrast, experimental data show a constant value at high velocities and larger ratios for negative-particle impact than for positive-particle impact.

Three decades ago, McGuire proposed that for direct double ionization of helium these inconsistencies could be resolved [3] if, in addition to the second-order independent-electron mechanism mentioned above (where $n = 2$), first-order mechanisms, such as those used to explain double ionization by photons, are considered. One first-order mechanism is shake-off (SO), where a large energy transfer ejects one of the target electrons with high speed without any subsequent interaction with any other target electron. This causes an abrupt change in potential of the target electronic cloud, which liberates a second electron with low energy. Quantum mechanically, SO is described by an overlap between the initial and final atomic states. Another first-order mechanism, commonly referred to as the two-step-one interaction (TS1), involves a low-energy transfer that ejects one of the target electrons. As this electron exits it knocks out a second electron; this is also known as interchannel coupling. Note, however, that in total-cross-section measurements there is a fundamental difference between double ionization resulting from photon and charged-particle impact, even if only first-order processes are considered. This is because in photoionization, excluding Compton scattering, the entire photon energy is deposited, whereas for charged particles a distribution of energies, depending on the impact parameter, is transferred. It turns out that the charged-particle impact ratio can be expressed as a weighted integral over the photon ratios at the various energies [4,5]. In fact, experimentally, the asymptotic photon ratio is about 1.7% [6], while the charged-particle ratio is 0.26% [7]. The other major difference is that the IEM does not

*Corresponding author: dubois@mst.edu

apply for photoionization because the photon only interacts once; hence the second-order interaction, often referred to as the two-step-two interaction (TS2) mechanism, does not exist.

McGuire pointed out that these first- and second-order mechanisms can interfere with the interference term being proportional to $(Ze/v)^3$. This is illustrated in Eq. (1) where the double-ionization cross section is written as the sum of a first- and a second-order cross section plus an interference term

$$\sigma_2 = \sigma_{1\mathrm{st}} + \sigma_{2\mathrm{nd}} + \sigma_{\mathrm{int}}. \quad (1)$$

In terms of scaled amplitudes these cross sections are defined as $[(Ze/v)A_{1\mathrm{st}}]^2$, $[(Ze/v)^2A_{2\mathrm{nd}}]^2$, and $2\cos(\varphi)(Ze/v)^3A_{1\mathrm{st}}A_{2\mathrm{nd}}$, respectively, where the A's are amplitudes and φ is the phase difference between the matrix elements corresponding to the first- and second-order mechanisms.

Dividing by the single-ionization cross section, a predominantly first-order process that scales as $(Ze/v)^2\ln(v)$ yields the ratio version of Eq. (1), namely, $R_2 = R_{1\mathrm{st}} + R_{2\mathrm{nd}} + R_{\mathrm{int}}$. Because of the different projectile charge and velocity dependences, this model predicts that for large Z/v, i.e., at lower velocities for a given Z, the second-order TS2 mechanism dominates and R_2 decreases approximately as $(Z/v)^2$, while for intermediate values of Z/v, i.e., at higher velocities for a given Z, the falloff is slower since the TS2 term decreases faster than the interference term does and as $Z/v \to 0$, corresponding to very high velocities, the first-order term dominates and R_2 approaches a constant value. In this model the phases are such that the cosine term is assumed to be positive because then the interference term R_{int} will be positive for negative Z and negative for positive Z, in agreement with the larger ratios that are observed for negative projectiles, i.e., for electrons and antiprotons, with respect to positive particles such as positrons, protons, and positive ions.

The McGuire paper stimulated numerous experimental investigations of double ionization where, to avoid complications resulting from inner-shell Auger processes, double ionization of helium was primarily studied and coincidence methods were often used in order to eliminate contributions associated with electron capture or loss by the projectile. A few examples include the work of Haugen *et al.* [8] and Knudsen *et al.* [9], who measured double- to single-ionization ratios for a number of different ions and energies with Z/v ranging from 0.1 to 3, with v in atomic units. Ullrich *et al.* [7] tested the high-velocity limit of R_2 by using relativistic bare neon and nickel ions with velocities ranging from ~40% to 90% the speed of light. In agreement with the findings of Knudsen *et al.*, they found that for larger Z/v the ratios increased as v^{-2} but were velocity independent as $Z/v \to 0$. Antiproton and proton impact data were compared [10–13] with the observed differences in the double ionization being attributed to quantum interference, in accordance with the McGuire model. For a synopsis of the antiproton and proton studies see [11] and references therein.

The McGuire paper plus the advent of antiproton impact data also stimulated numerous theoretical studies and have produced various explanations for the physical mechanisms responsible for the features described above. For example, the observed differences in the double ionization have been attributed to different ionization probabilities, depending on the sign of the projectile charge, at small impact parameters [14,15]; to the Z^3 term, in accordance with the interference model of McGuire [16]; to the two electrons being removed in uncorrelated events at different internuclear distances [17,18]; and to electron correlation in the initial and final states [1,19,20]. In general, all of these models yielded reasonable agreement at high energies, but overestimated the cross sections at lower energies. So Kirchner *et al.* [21] addressed the low-energy problem and showed that the inclusion of target polarization and binding effects reduced both the single- and double-ionization cross sections for antiproton impact at low energies, but not enough to match the experimental data. They attributed the remaining discrepancies to the lack of correlation in their model. A different model based up the strong electric field of the projectile leading to ejection or capture of target electrons has also been proposed [22,23], but its range of application should be limited to regions where Z/v is large and, in contrast to the McGuire and several other models, has no explicit first-order and second-order interference contributions to explain the observed differences in double ionization resulting from positive- and negative-projectile impact.

Therefore, many different theoretical approaches have been tried and various explanations have been offered with regard to the observed velocity dependences for double ionization and why double ionization is larger at low and intermediate energies for negatively charged projectile impact than it is for positively charged projectiles. However, all of these comparisons have been hampered in several ways. First, in most cases only select systems have been modeled, e.g., typically only proton and antiproton data or only low-Z positive-ion data. Second, in certain cases only the second-order mechanism has been modeled with the corresponding first-order mechanism and any possible interference contributions lacking. Third, when both first- and second-order contributions have been included in the theoretical models, we are aware of only one or two cases where results for the individual contributions have been presented. Almost exclusively only the overall sum has been compared with experiment simply because experimental information about the individual components is lacking, at least at the integral cross-section level.

This work addresses these problems within the context of the first- and second-order interference model of McGuire and is a follow-up of an earlier study where, based upon observed velocity dependences, we concluded that first-order double-ionization processes dominated for $Z = 1$ projectiles [24,25]. Here we show that this interpretation was incorrect and that the observed velocity dependence is significantly influenced by the large interference contribution for proton and antiproton impact. The present work shows that all existing data for direct double ionization of helium by bare ions are consistent with the first- and second-order interference model of McGuire. More importantly, the present study provides quantitative information and predictions about contributions of the first- and second-order double-ionization channels as well as for the interference term for a wide range of systems and energies. This is achieved by extracting empirical scalings for the various contributions to double ionization plus information about the phase difference between the first- and second-order

mechanisms from experimental data. The empirical formulas we obtain can be used to (a) guide theory by showing which process needs to be modeled, (b) indicate where interference needs to be included and where it can be ignored, (c) provide quantitative predictions for the individual double-ionization mechanisms that can be individually compared with various theoretical models, or (d) simply test the reliability of existing or new data.

II. ANALYSIS PROCEDURE

Our analysis is based on a large database of published experimental cross sections and double-ionization ratios [7–13,26–38]. To simplify the interpretation, only data for the direct ionization channel, i.e., only data where there are no contributions from the electron-capture channel, and fully stripped projectile impact were used. Also, where multiple sets of data are available for a particular ion, we have arbitrarily selected only one that we consider to be representative and reliable. Figure 1 shows how the measured double- to single-ionization ratios of helium R_2 vary as a function of impact velocity v for fully stripped ions ranging from protons to bare krypton, U^{90+}, and for antiprotons. As illustrated by the proton and neon data, when Z/v is small, i.e., Z is small and/or v is large, the ratios are in near agreement with the theoretical shake limit (see Ref. [7]) shown by the arrow on the right-hand axis. However, as Z/v becomes large the ratios increase approximately as v^{-2}, as shown by the solid line through the He^{2+} data. This increase was attributed to the second-order mechanism becoming dominant. However, for proton and antiproton impact, Fig. 1 shows a dependence more consistent with a v^{-1} behavior, as shown by the dashed line through the proton data. We recently noted this [24,25] and attempted to interpret the proton and antiproton data solely in terms of the first-order SO and TS1 mechanisms, which were assumed to interfere. We note that Shao *et al.* also found a v^{-1} behavior for conditions where $Z/v > 1$ [22,23].

To investigate the different velocity dependences for the $Z = 1$ and higher-Z projectiles, plus to fully test the first- and second-order interference model of McGuire, the experimental asymptotic high-energy ratio, which is assumed to be entirely first order, $R_{1st}(\infty) = 0.002\,59$ [7], was subtracted from each experimental R_2 value in Fig. 1. We note parenthetically that this experimental ratio agrees essentially exactly with the theoretical first-order i.e., shake, ratio for large v [39]. Here we reiterate that the shake ratio for charged-particle impact is considerably smaller than that for photon impact, as mentioned above. This is because the photon deposits its entire energy, whereas for charged particles, a distribution of energies that depend on the impact parameter is transferred. For ion impact, the mean energy transfer is on the order of 20–30 eV and is relatively independent of impact energy [40]. Thus, $R_{1st}(\infty)$ for charged particles should be approximately the same as $R_{1st}(h\upsilon \sim 30\,\text{eV})$ for photon impact, which it is [41]. Also, because the energy transfer is approximately constant and because Fig. 1 shows that with decreasing velocity the measured ratios are considerably larger than their asymptotic limit, subtracting a constant value is reasonable. According to the ratio version of Eq. (1), this subtraction should isolate the second-order plus interference contributions $R_{2nd} + R_{int}$ if the McGuire model is applicable.

After subtracting $R_{1st}(\infty)$, it was found that the maxima clearly observed for the $Z = 2$ to 9 data in Fig. 1 could be normalized together by dividing $R_2 - R_{1st}(\infty)$ by $Z^{6/5}$ and v by $Z^{2/5}$. As can be seen in Fig. 2, after subtracting a constant first-order contribution and scaling both the ratios and velocities, the higher-velocity dependences of $R_{2nd} + R_{int}$ for $Z > 1$ are consistent with a second-order process being dominant, e.g., either $1/v^2$ or $1/[\ln(v)v^2]$. Thus, the scaled velocity dependence, i.e., $(v/Z^{2/5})^{-2}$, combined with the scaled ratio dependence yields the expected IPM cross-section scaling, namely, $\sigma_n \sim (Z/v)^{2n}$. Further support of a dominant second-order mechanism is the strong similarity between the scaled second-order plus interference contributions and

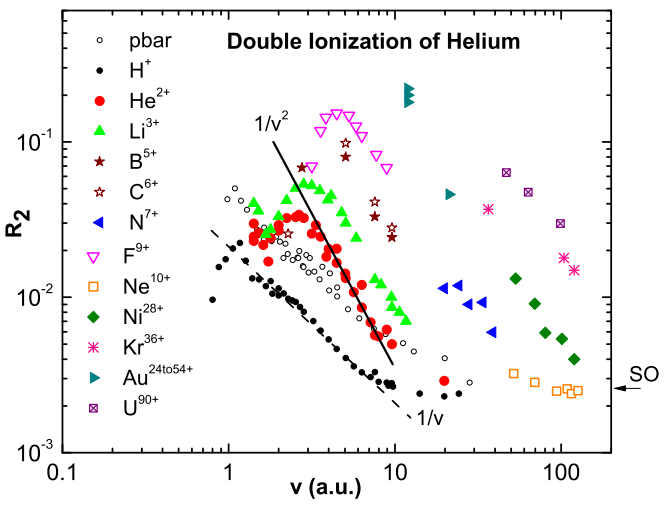

FIG. 1. (Color online) Measured ratios for double ionization of helium by bare ion impact as a function of impact velocity in atomic units. Data are from Refs. [7–13,28–40]. The lines illustrate v^{-1} and v^{-2} velocity dependences.

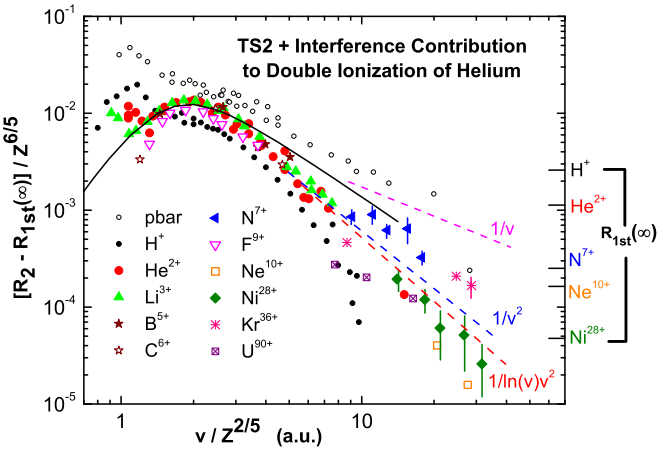

FIG. 2. (Color online) Scaled second-order plus interference contributions to the double-ionization ratios in Fig. 1. Data sources are the same as in Fig. 1. The dashed lines illustrate v^{-1}, v^{-2}, and $[\ln(v)/v^2]^{-1}$ velocity dependences while the solid line shows normalized single-ionization cross sections from Ref. [42]. Scaled values for $R_{1st}(\infty)$ are shown at the right axis.

normalized cross sections for direct, predominantly single, ionization of helium by protons [42], shown by the solid black curve in Fig. 2. Finally, the larger and smaller ratios for antiproton and proton impact imply strong interference effects, in accordance with the McGuire model. Also, because all positive ions except protons are shown to scale, the proton and antiproton differences cannot be explained simply by differences in target polarization or distortion due to the sign of projectile charge as was suggested in [20]. The reader should note that some of the proton data around 10 a.u. and a few of the Ne^{10+} data points from Fig. 1 are missing in Fig. 2 since the subtraction yielded negative values, which cannot be shown on a logarithmic scale. Also note that scaled asymptotic values, denoted by $R_{1st}(\infty)$, are indicated at the right-hand axis in order to illustrate the relative importance of the first- and second-order mechanisms as Z increases.

Ionization by protons and antiprotons

To study the dependences shown in Fig. 2 in more detail, experimental cross sections for single and double ionization by antiprotons and protons [9,13,26,27,36] were investigated. These cross sections were fitted with simple functions in order to provide scaling formulas for the first and second order and for the interference contributions to double ionization. The scaling formulas were then used to calculate double- to single-ionization ratios, which can be compared to the experimental data in Figs. 1 and 2.

Rather than the more complex procedures and formulas recently presented for determining ionization by any projectile [43], we fit the single-ionization data with simple functions of the form $C_{lo}v^m$ below the cross-section maxima and $C_{hi}f(v)$ above the maximum. Here C_{lo}, C_{hi}, and m are fitting parameters and $f(v)$ is the velocity dependence well above the maxima, e.g., $\ln(v)/v^2$. The overall fit was the combination of these functions, e.g., $[\{C_{lo}v^m\}^{-1} + \{C_{hi}f(v)\}^{-1}]^{-1}$. This required extending the high function to scaled velocities less than 1, therefore a constant k was added in the logarithmic term to avoid negative logarithmic values that prohibited achieving a good fit in the low-velocity region. Thus, for single ionization, $f(v) = \ln(k+v)/v^2$. Using $k = 0.4$, $C_{lo} = 0.375$, $m = 4$, and $C_{hi} = 4.75$, a good fit to the proton data was obtained. Based upon the latest data [13], near the cross-section maximum (e.g., ~100 keV) the single-ionization cross sections for antiproton impact are approximately 20% smaller than for proton impact, but become significantly larger than for proton impact for energies less than 25 keV. A good fit to the antiproton data in the low-energy region was achieved for $C_{lo} = 0.65$ and $m = 1.5$. Note that in fitting the proton data, the early single-ionization measurements of Afrosimov *et al.* [36] were not included as they are significantly larger than cross sections measured by Shah *et al.* [27] and the total cross sections of Rudd *et al.* [42].

The double ionization is more complex since Eq. (1), the McGuire model, shows that three terms contribute. We obtained information about the individual terms plus about the phase difference ϕ between the first- and second-order mechanisms in the following manner. Although the Born approximation implies that the first- and second-order amplitudes are the same for proton and antiproton impact, as stated above, experimental data show small differences, on the order of 20% or less, for velocities between approximately 1 and 3. Therefore, according to the definitions of the terms and Eq. (1),

$$\sigma_2(\text{proton}) = \sigma_{1\text{st proton}} + \sigma_{2nd} - \sigma_{int}, \tag{2a}$$

$$\sigma_2(\text{antiproton}) = \sigma_{1\text{st antiproton}} + \sigma_{2nd} + \sigma_{int}, \tag{2b}$$

and

$$\sigma_{int} = 2\cos(\varphi)[\sigma_{1st}\sigma_{2nd}]^{1/2}. \tag{2c}$$

Therefore, adding and subtracting Eqs. (2a) and (2b) isolates σ_{2nd} and σ_{int}; combining the results will yield the phase information, e.g.,

$$\sigma_{2nd} = [\sigma_2(\text{antiproton}) + \sigma_2(\text{proton})]/2 - \sigma_{1\text{st av}} \tag{2d}$$

and

$$\cos(\varphi) = [\sigma_2(\text{antiproton}) - \sigma_2(\text{proton})]/4[\sigma_{1\text{st av}}\sigma_{2nd}]^{1/2}, \tag{2e}$$

where $\sigma_{1\text{st av}}$ is the average of $\sigma_{1\text{st proton}}$ and $\sigma_{1\text{st antiproton}}$. Note that it is also possible to use double- to single-ionization ratios, rather than cross sections, in Eqs. (2). For the cross-section version, σ_{1st} is obtained from $R_{1st}(\infty)\sigma_1$. As stated previously, we expect this to be reasonably accurate except perhaps at lower velocities where, in any case, $\sigma_{2nd} \gg \sigma_{1st}$. Here σ_{2nd} can also be obtained by multiplying R_{2nd} by σ_1 with R_{2nd} being obtained from the ratio version of Eq. (2d).

Figure 3 shows σ_{2nd} determined directly by adding the proton and antiproton double-ionization cross sections (closed squares) and indirectly by adding their double-ionization ratios and multiplying the result by the experimental single-ionization cross sections (open squares). Fitting σ_{2nd} with the same functional forms as for single ionization yielded constants for the low region of $c_{lo} = 0.008$ and $m = 2$. For the high region, a fit using $f(v) = v^{-n}$ yielded n between 3 and 3.5, which is significantly slower than the v^{-4} dependence

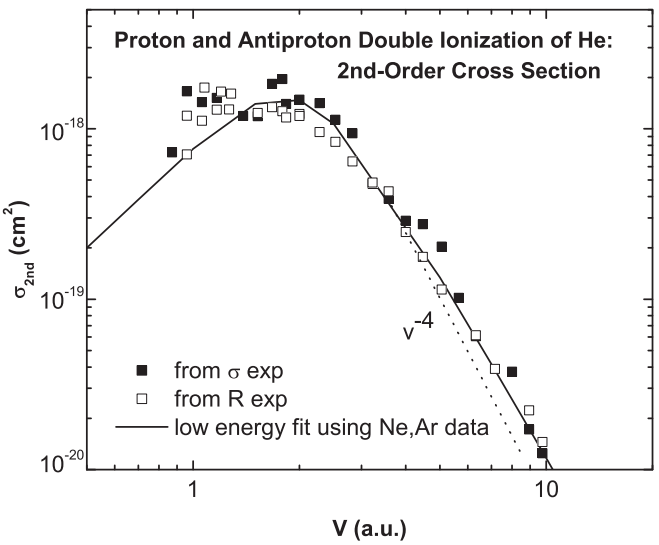

FIG. 3. Second-order cross section σ_{2nd} obtained from adding proton and antiproton impact double-ionization cross sections from Refs. [8–13,26,27,36]. The solid line is a fit with a high-velocity dependence of $\ln(v)v^{-4}$ while the dashed line illustrates a high-velocity v^{-4} dependence.

suggested by McGuire for a second-order process. However, if a sequential two-step double-ionization process is assumed, where the first electron is ionized via a distant interaction, which scales as $\ln(v)/v^2$, followed by a second, closer, interaction that liberates the second electron and scales as v^{-2}, a slower falloff of $\ln(v)/v^4$ is predicted. This is in good agreement with the experimental data, as shown in Fig. 3, and supports the theoretical model used in Ref. [17]. The solid curve in Fig. 3 has a high-velocity dependence of $f(v) = \ln(0.4 + v)/v^4$ and uses a constant of $c_{\rm hi} = 0.5$ with the low dependence as defined above. As before, the logarithmic term has been modified in order to extend to velocities less than 1. The dotted curve showing a v^{-4} dependence is provided for comparison purposes.

Figure 4 shows cosines of the phase difference between the first- and second-order mechanisms that were extracted from the experimental double-ionization ratios combined according to the ratio equivalents of Eqs. (2d) and (2e). Cosines were also calculated using double-ionization cross sections, but are not shown as the number of energies where both proton and antiproton cross sections are available was smaller, plus where information was available, the scatter in the data was significantly larger. The fitted line to the data shown is given by $\cos(\phi) = 0.35 + 0.4v^{-2}$.

After rewriting our fitting formulas for proton and antiproton impact ionization of helium, our analysis yields the following models and fits to the data: For single ionization,

$$\sigma_1 = [1 + (C_{\rm hi}/C_{\rm lo})\ln(k + v)/v^{2+m}]^{-1} C_{\rm hi}\ln(k + v)/v^2. \quad (3a)$$

For double ionization,

$$\sigma_{\rm 1st\ order} = R_{\rm 1st}(\infty)\sigma_1 = 0.002\,59\sigma_1, \quad (3b)$$

$$\sigma_{\rm 2nd\ order} = [1 + (c_{\rm hi}/c_{\rm lo})\ln(k + v)/v^{4+m}]^{-1} c_{\rm hi}\ln(k + v)/v^4, \quad (3c)$$

where

$$\sigma_{\rm int} = 2\cos(\phi)[\sigma_{\rm 1st\ order}\sigma_{\rm 2nd\ order}]^{1/2} \quad (3d)$$

and

$$\cos(\phi) = 0.35 + 0.4v^{-2}, \quad (3e)$$

with the maximum value being 1. For proton and antiproton impact and velocities in atomic units, in units of $10^{-16}\,{\rm cm}^2$, Eq. (3a) yields single-ionization cross sections using $C_{\rm hi} = 4.75$, $k = 0.4$, $C_{\rm lo} = 0.375$ (proton), $C_{\rm lo} = 0.65$ (antiproton), $m = 4$ (proton), and $m = 1.5$ (antiproton) and Eqs. (3b)–(3e) yields double-ionization cross sections using $c_{\rm hi} = 0.5$, $c_{\rm lo} = 0.008$, and $m = 2$. These cross sections for single and double ionization of helium by protons and antiprotons, plus cross-section ratios, obtained using these formulas and constants are compared with experimental data in Fig. 5. The solid black curves for single ionization are obtained using Eq. (3a) and the constants listed above. For double ionization, the solid red (upper) and blue (lower) curves are total cross sections obtained by adding the first-order (dashed magenta curve), second-order (dashed black curve), and interference (dotted green curve) cross sections shown. Note that here σ_{1st}, $\sigma_{\rm int}$, and $\sigma_{\rm 2nd}$ were determined using the fit to the proton single-ionization cross sections, which for $v > 1$ introduces changes less than 10% from values obtained using $\sigma_{\rm 1st\ av}$. Doing so allowed us to determine these quantities in Fig. 5 using only experimental data. Overall, good agreement with measured values is achieved except at the lowest velocities where the early proton impact measurements of Afrosimov *et al.* [36] are significantly smaller while the antiproton data are larger than our analysis and fits predict. This might imply problems with the low-energy double-ionization data. Or it could imply that higher-order processes need to be included since we have extended our analysis and fits to very low velocities. Another possibility for the discrepancy at low energies is

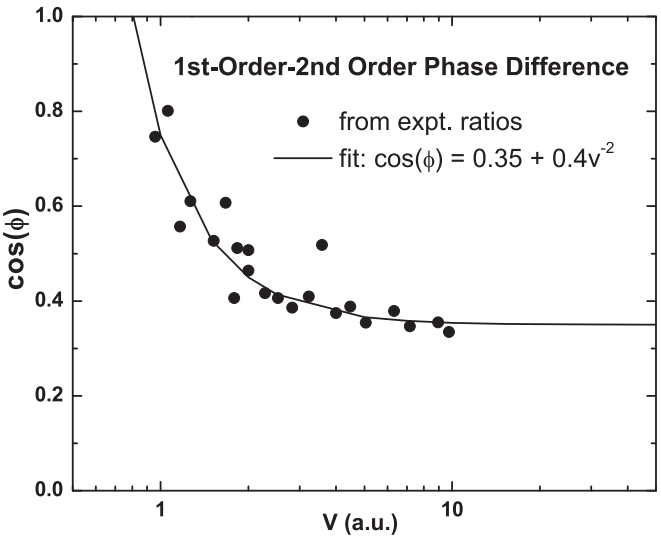

FIG. 4. Cosines of the phase difference between the first- and second-order ionization mechanisms obtained from subtracting proton and antiproton impact double-ionization cross sections. The data are the same as in Fig. 3. The solid line is a fit.

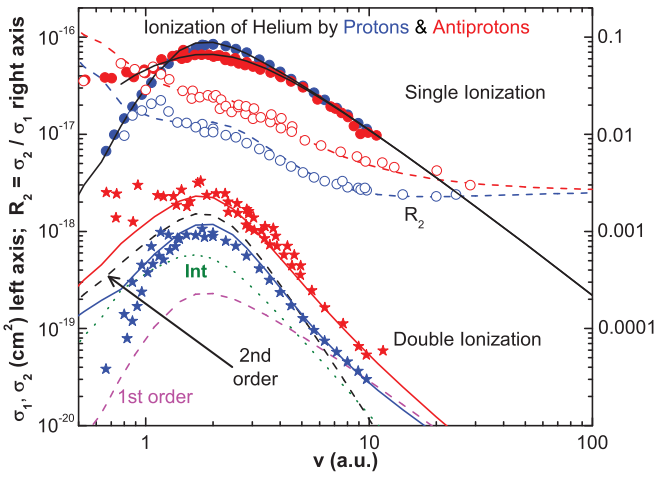

FIG. 5. (Color online) Predictions for the various channels leading to single and double ionization of helium by protons and antiprotons, plus double- to single-ionization ratios, obtained using Eqs. (3) and our fitting parameters compared to experimental data from Refs. [8–13,26,27,36]. The dotted curves show $\sigma_{\rm int}$ and σ_2 determined using the fit to the antiproton single-ionization cross sections.

that our method of calculating $\sigma_{1\text{st order}}$ by multiplying σ_1 by $R_{1\text{st}}(\infty)$ is too simplistic. For example, note that if the TS1 mechanism is velocity dependent and decreases with impact velocity, both the first-order and the interference terms would be underestimated at low velocities, thus leading to an overestimation for proton impact and an underestimation for antiproton impact, as shown in Fig. 5.

The present data and analysis indicate that the second-order mechanism dominates at lower velocity and that interference between the first- and second-order double-ionization mechanisms accounts for differences between proton and antiproton impact, as predicted by the McGuire model. In the high-velocity region, our analysis implies that near $v = 10$ the first- and second-order mechanisms are approximately equal in magnitude but opposite in sign for proton impact, thus canceling their contributions for proton impact. This is not the case for antiproton impact where the signs of the matrix elements for the first- and second-order mechanisms are the same; thus inclusion of the interference term increases the double-ionization cross section by a factor of 2 near $v = 10$ a.u. The effects of this cancellation versus enhancement are clearly shown in Fig. 2. For proton impact velocities greater than 10, σ_{int} is larger than $\sigma_{2\text{nd}}$ which, because σ_{int} is negative, means R_2 in this region is smaller than at the asymptotic limit. Overall, reasonable qualitative agreement with measurements is achieved for the cross-section ratios, even at low velocities where the proton and antiproton impact ratios increase rather than decrease, as shown in Fig. 2 for multiply charged ion impact. The present analysis implies that this increase is due to the different velocity dependences in the threshold region for single and double ionization, although we cannot rule out contributions from higher-order terms.

Figure 6 shows a comparison of our empirical curves for the SO and TS2 mechanisms with the *ab initio* calculations of Gulyás *et al.* [1] and Nagy *et al.* [18] As can be seen, the agreement is typically better than 30%, with the time-ordered model of Nagy *et al.* yielding somewhat better agreement. However, the present work plus the calculations of Gulyás *et al.* imply that the SO contributions of Nagy *et al.* are too small at lower velocities. In addition, for these lower velocities the interference contribution that we obtain is larger than that quoted by Nagy *et al.*, which may explain why their calculated values for proton impact are too large plus why their model gave approximately the same cross section for double ionization by protons and antiprotons.

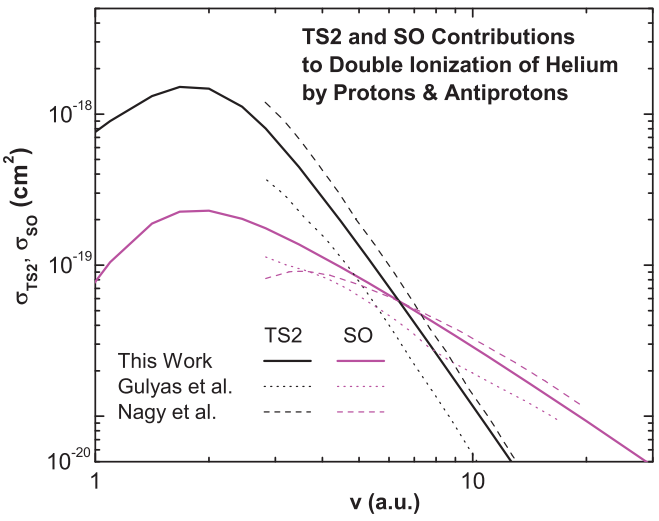

FIG. 6. (Color online) Cross sections for the TS2 and SO contributions to double ionization of helium by protons and antiprotons. Thick solid lines represent the present work; thin solid lines with dots, Gulyás *et al.* [1]; and dashed lines, Nagy *et al.* [18].

III. IONIZATION BY BARE MULTIPLY CHARGED IONS

To extend our analysis to multiply charged ion impact, experimental cross sections for He^{2+} [9,26–28,38], Li^{3+} [26,29], F^{9+} [31], and U^{90+} [34] impact were used. Guided by the scaling found in Fig. 2, the cross sections were divided by $Z^{(6/5)n}$, where $n = 1,2$ for single and double ionization, respectively, and the impact velocities were divided by $Z^{2/5}$. To more directly test the scaling of the second-order contribution to double ionization, the first-order contribution was subtracted before applying this scaling. Figure 7 shows that these scalings bring the data into near agreement with each other, although the double-ionization data seem to indicate that scaling by $Z^{12/5}$ works well for low Z but is too large for higher-Z ions. The few outlying points around scaled velocities of unity are the early measurements of Afrosimov *et al.* [38], which are in qualitative, but not quantitative, agreement with more recent, and presumably more accurate, measurements.

Applying these scalings to Eqs. (3a) and (3c), i.e., multiplying by $Z^{(6/5)n}$ and replacing v with $v/Z^{2/5}$, yields the orange dotted curves in Fig. 7. These can be seen to decrease too slowly in the low region. By increasing the velocity power m by 2 for both single and double ionization, e.g., to 6 and 4, respectively, and using $C_{\text{lo}} = 0.35$ and $c_{\text{lo}} = 0.0035$ with C_{hi}

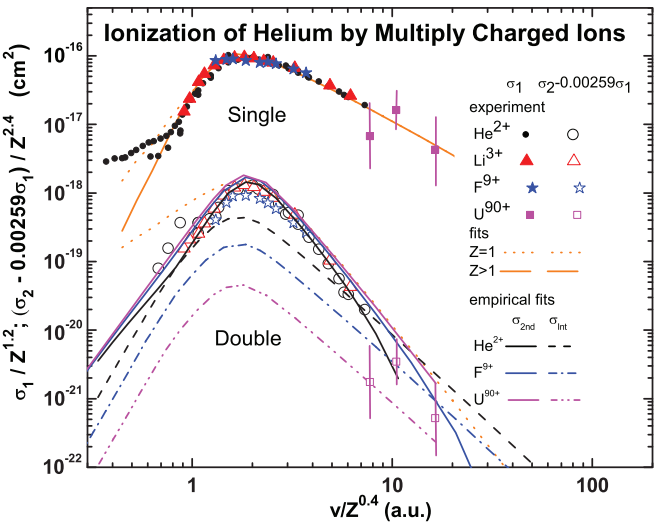

FIG. 7. (Color online) Predictions for σ_1 plus $\sigma_{2\text{nd}}$, σ_{int}, and their sum for ionization of helium by He^{2+}, F^{9+}, and U^{90+} obtained by scaling Eqs. (3) and using the fitting parameters for multicharged bare ions, e.g., $C_{\text{hi}} = 4.75$, $k = 0.4$, $C_{\text{lo}} = 0.35$, $m = 6$, $c_{\text{hi}} = 0.5$, $c_{\text{lo}} = 0.0035$, and $m = 4$. The dotted curves are made using the fitting parameters. The experimental data are for He^{2+}, Li^{3+}, F^{9+}, and U^{90+} ions from Refs. [9,26–29,31,34,38].

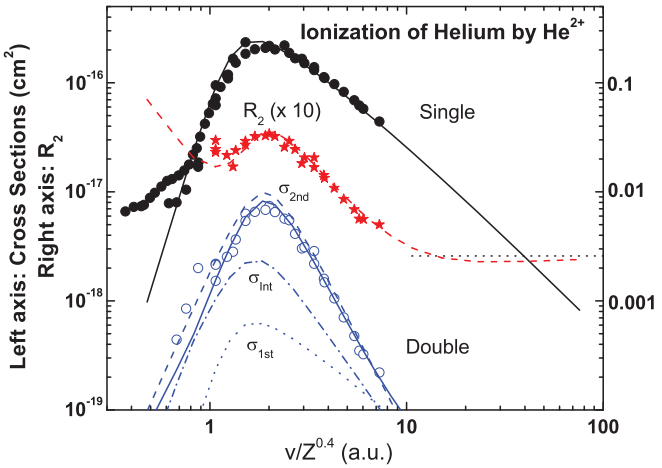

FIG. 8. (Color online) Predictions compared to experimental values for single and double ionization of helium by He^{2+} ions. Data are the same as in Fig. 7.

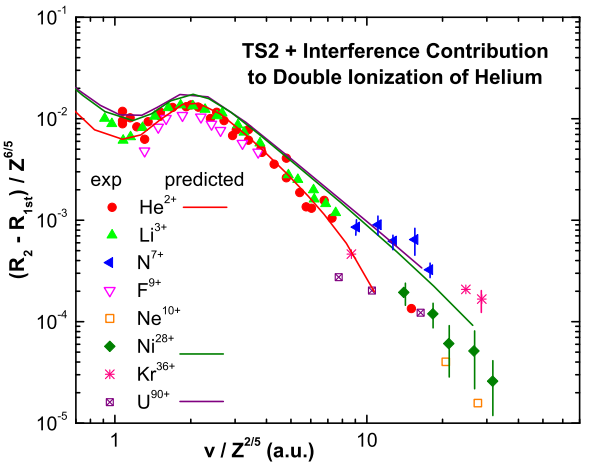

FIG. 9. (Color online) Predictions compared to experimental values for the second-order plus interference contributions to double ionization of helium by bare ions. Data are the same as in Fig. 2.

and $c_{\rm hi}$ unchanged, a good match to the data, as shown by the solid orange curves, is obtained. Equation (3b) provided values for σ_{1st}. Then, with the assumption that the phase differences between first- and second-order terms in the transition matrix element are the same for all projectiles, $\sigma_{\rm int}$ was calculated from Eq. (3d) and is shown by the dashed and dot-dashed curves. As can be seen, our predicted cross sections are in relatively good agreement with experimental data, although there is a systematic overestimation by our predictions as Z becomes large.

Figure 7 illustrates the decreasing importance of the interference term with increasing Z. Using our fitting formulas and parameters, we predict the relative importance of $\sigma_{\rm int}/\sigma_{\rm 2nd\,order}$ in the higher-velocity region to be approximately $\frac{1}{6}v_{\rm sc}Z^{-3/5}$, where $v_{\rm sc} = v/Z^{2/5}$. Thus, for $Z = 1$,2,9 between $v_{\rm sc} = 2$ and 6 our analysis predicts the relative importance of $\sigma_{\rm int}$ with respect to $\sigma_{\rm 2nd\,order}$ to be approximately 0.3 to 1 ($Z = 1$), 0.2 to 0.7 ($Z = 2$), and 0.08 to 0.25 ($Z = 9$). The strong relative importance for protons and antiprotons plus the relative insignificance for higher-Z ions explains the scaling behavior and different velocity dependences shown in Fig. 2 plus why we originally misinterpreted the mechanisms leading to double ionization [24,25].

Closer looks at the predictions based on our analysis and scalings are shown in Figs. 8 and 9. Figure 8 shows that our predicted values are in excellent agreement with measurements for He^{2+} impact. Using selected multiply charged ion data, Fig. 9 compares predictions from our fits and scaling with ratios where the first-order contributions have been removed. For small Z our predicted values are in excellent agreement and reproduce the dip seen for scaled velocities near 1. For high-Z ions, our predictions are in qualitative agreement but are roughly 50% too large. We attribute the overestimation to a breakdown of the Z scaling that was used. Based upon interpolations of the ionization probabilities calculated for proton impact as a function of impact parameter [15], applying a Z^2 scaling yields maximum double-ionization probabilities greater than 0.2 for U^{90+} and Ni^{28+} ions having impact velocities smaller than ~20 and 10 a.u., respectively, i.e., for scaled velocities in Fig. 8 less than 4–6 a.u. This breakdown in scaling, due to either a large Z or a small v, means that higher-order terms become important, which if additive would be consistent with the increasing overestimation of our calculated ratios observed for F^{9+}, Ni^{28+}, and U^{90+} impact. Based upon the good agreement found for antiproton calculations down to $v \sim 0.25$, where only a second-order expansion was used [17], and the good scaling seen in Fig. 9, we do not expect higher-order terms to be important for $Z < 9$ except perhaps for the lowest scaled velocities.

Extension to other targets

As illustrated above, our analysis provides cross-section formulas for the various channels contributing to double ionization of helium that are in reasonable agreement with experimental measurements for fully stripped ions and most impact velocities. To take this analysis one step further, we investigated whether the formulas also apply, or can be modified, for double outer-shell ionization of other atoms. For this purpose, single- and double-ionization cross sections for proton, antiproton, and multiply charged ion impact on helium, neon, and argon were used (He target references are provided above, Ne target data are from Refs. [12,28,36], and Ar target data are from Refs. [11–13,26,27]). For single ionization, the target scaling formula presented by Montenegro *et al.* [43,44] combined with our projectile scaling was applied. Thus, σ_1 was divided by $Z^{6/5}\delta_1 N/I_1^2$ and the impact velocity v was divided by $Z^{2/5}I_1^{1/2}$. Here δ_1 is a number on the order of unity used to account for changes in the dipole matrix element for different targets and subshells, N is the number of outer-shell electrons (2 for He and 6 was used for Ne and Ar), and I_1 is the first-ionization potential in atomic units. For double ionization, based upon our assumption that a distant interaction followed by a closer interaction takes place, we applied the scaling of Montenegro *et al.* twice where for the first ionization the parameters were identical to those used for single ionization, while for the second ionization it was assumed that the first

electron was already far away, meaning a different value for δ_1, one fewer electron, and the second-ionization potential were required. Note that this method is analogous to the time-ordered model of Nagy *et al.* [18]. Therefore, σ_2 was divided by $(Z^{6/5}\delta_1 N/I_1^2)(Z^{6/5}\delta_2\{N-1\}/I_2^2)$. This means that for different targets $R_{2\mathrm{nd}}$ should scale as $Z^{6/5}\delta_2\{N-1\}/I_2^2$. For the velocity scaling, it is unclear from our assumptions whether scaling by I_1, I_2, I_1+I_2, or $(I_1+I_2)/2$ should be used. All were tested with I_1 yielding the best overall compression for proton and antiproton impact. For multicharged ion impact, it was found that scaling the helium target velocities by I_1 and the neon and argon velocities by I_2 was required, which we assume must have something to do with the fact that Ne and Ar are multishell atoms.

Based upon total-cross-section data, Montenegro *et al.* provided values for δ_1, namely, 0.8 for ionization of He and 0.5 for Ne and Ar [43,44]. We used the recommended value for He and adjusted the values for Ne and Ar slightly to provide a better overall compression of the σ_1 data to a single curve. Assuming that both δ_1 and δ_2 are 0.8 for ionization of He, values of δ_2 for Ne and Ar were adjusted to give the best overall compression of the double-ionization cross sections as well as for the cross-section ratios. Since our primary goal was to investigate how similar double outer-shell ionization of these different targets is, best values for δ_2 were determined independently for ionization by protons, antiprotons, and multiply charged ions.

Figure 10 shows the results and the parameters used. The upper curves in each figure are scaled experimental single-ionization cross sections compared with our scaled Eq. (3a). For proton impact, the scaling is quite good. For antiproton impact an increasing deviation can be seen at lower velocities. For multicharged ion impact, the scaled data differ by roughly a factor of 2 near the cross-section maxima.

The lower curves are estimates of the second-order plus interference contribution to the double-ionization ratios compared to the same values determined from scaled versions of Eqs. (3). In both cases, $R_{1\mathrm{st}}(\infty)$ has been subtracted. Since the measured double-ionization ratios for neon and argon include contributions from inner-shell ionization, the outer-shell contribution was estimated by multiplying $R_{1\mathrm{st}}(\infty)$ for helium by our target scaling formula for single ionization. This yielded values of 0.0123 for Ne and 0.0234 for Ar as compared to the measured values of 0.0295 and 0.0628 [45] with the difference being attributed to inner-shell ionization. For neon, better agreement with the data was found by using 0.018 rather than 0.0123. Using these values plus values for δ_2 shown in the insets, Fig. 10 shows strong similarities in the second-order contributions to double ionization, except in the low-scaled-velocity regime for proton and antiproton impact. This could indicate problems with the experimental data or it could mean that addition double-ionization mechanisms are becoming important. Higher-order terms are obvious choices for additional mechanisms. However, the data do not show the strong increase in the ratios that would be expected from the inclusion of higher-order terms at low velocities. New measurements and theoretical studies concentrating on impact energies below the cross section maxima are needed to resolve this. As a final comment, the deviations seen for the proton and antiproton impact double-ionization ratios for argon at scaled

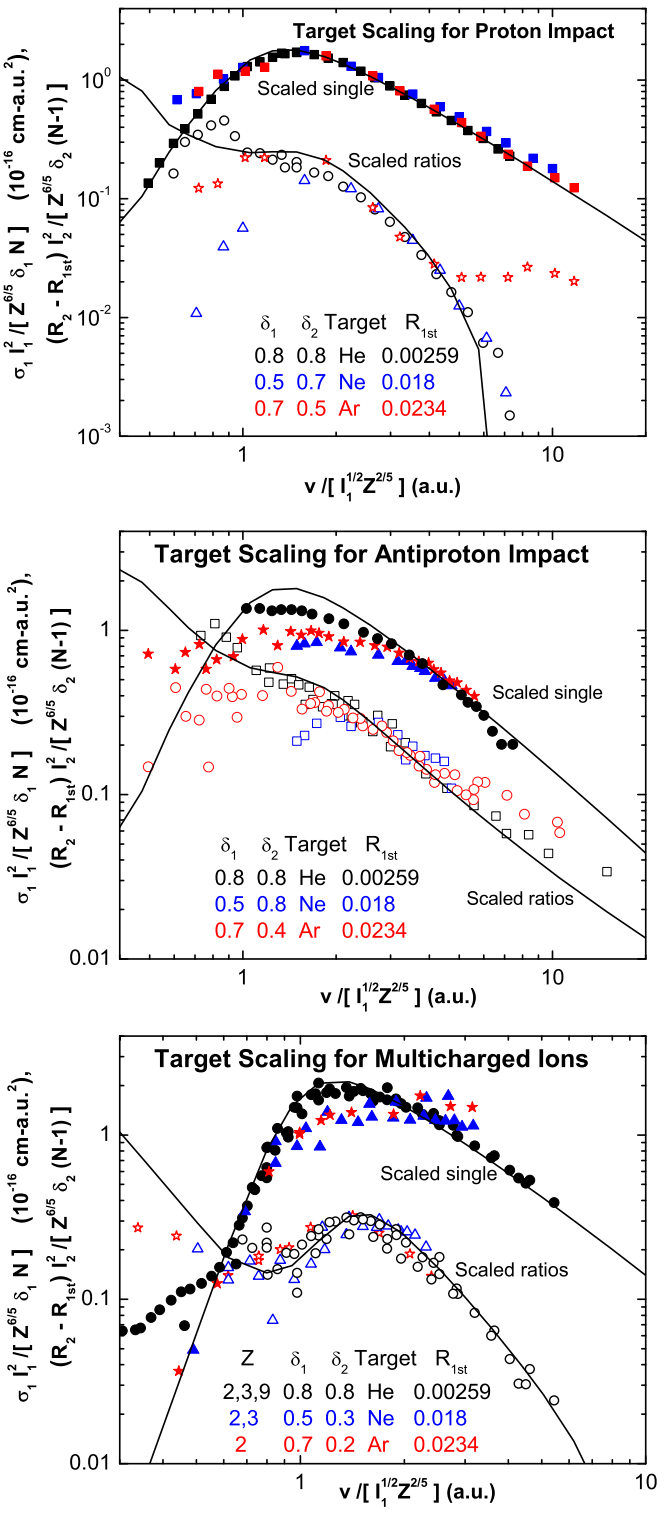

FIG. 10. (Color online) Scaled single-ionization cross sections and the second-order plus interference contributions to R_2 for proton (top graph), antiproton (middle graph), and He^{2+}, Li^{3+}, and F^{9+} (bottom graph) direct ionization of helium, neon, and argon. The curves are determined using Eqs. (3), the parameters listed in the figures, and the target and projectile scaling described in the text.

velocities greater than 5 indicate the inner-shell ionization channel becoming important. Therefore, with the exception of the low-velocity regime, Fig. 10 strongly implies that the

formulas provided here, when scaled, also apply for double outer-shell ionization of more complex atoms.

IV. SUMMARY AND CONCLUSIONS

Empirical formulas for single and double ionization derived by fitting experimental ionization cross sections and cross-section ratios for a wide range of systems and impact energies have been presented. Within the first- and second-order interference model of McGuire, analytical formulas for the various channels leading to single and double ionization as well for the phase difference between the matrix elements for first- and second-order ionization mechanisms were developed. At higher velocities the formulas for the TS2 and SO mechanisms were shown to be in good agreement with *ab initio* calculations available for proton impact. Multicharged ion data were used to extract projectile Z scaling dependences while proton, antiproton, and multicharged ion data for He, Ne, and Ar targets were used to extract target scaling dependences.

The present analysis supports the McGuire model for double ionization and shows that protons do not fit the same scaling found for all other positive ions because the interference term is more important over a broader velocity region for protons, as compared to higher-Z positive ions, owing to the different Z dependences of the first- and second-order mechanisms. Thus, the experimental data demonstrate that, in a general sense, the McGuire model is consistent with the differences in proton vs antiproton results. As the present fits are empirical in nature we cannot rule out contributions from higher-order terms at lower velocities. However, to explain the observed velocity dependences, either the higher-order contributions to double ionization must be weak with respect the second-order term or they must tend to cancel each other. It is certainly true that correlation and/or polarization effects should engender some changes in the second-order (and thereby the interference) term in the double- to single-ionization ratio, but the experimental data appear to suggest that differing polarization and/or correlation effects for proton vs antiproton projectiles are not of crucial importance. Furthermore, it was shown that a combination of these scalings and formulas provide very good to reasonable agreement for double outer-shell ionization of any atom by any fully stripped projectile for most impact velocities. Extension to partially stripped ion impact was not attempted as these systems are more complicated in that partial screening of the nuclear charge and elimination of projectile excitation accompanying target ionization must be taken into account and this is difficult to do.

These empirical formulas and scalings presented here can be used to guide theoretical treatments of double ionization by showing what mechanisms are important, or may be ignored, and whether interference effects play major or minor roles. They can also be used to help evaluate the reliability of various experimental data, especially in regimes where the data are difficult to measure. Finally, our analysis indicates the need for experimental and theoretical studies for scaled impact velocities less than unity.

ACKNOWLEDGMENT

This work was supported by the National Science Foundation, the Department of Energy, Office of Chemical Sciences, CNPq, and the Brazil-U.S. Physics Professorship/ Lectureship Program.

[1] L. Gulyás, A. Igarashi, and T. Kirchner, Phys. Rev. A **86**, 024701 (2012).
[2] C. C. Montanari, J. E. Miraglia, W. Wolfe, H. Luna, A. C. F. Santos, and E. C. Montenegro, J. Phys.: Conf. Ser. **388**, 012036 (2012).
[3] J. H. McGuire, Phys. Rev. Lett. **49**, 1153 (1982).
[4] S. T. Manson and J. H. McGuire, Phys. Rev. A **51**, 400 (1995).
[5] J. Wang, J. H. McGuire, J. Burgdörfer, and Y. Qiu, Phys. Rev. A **54**, 613 (1996).
[6] J. H. McGuire, Adv. At. Mol. Phys. **29**, 217 (1992), and references therein.
[7] J. Ullrich, R. Moshammer, H. Berg, R. Mann, H. Tawara, R. Dorner, J. Euler, H. Schmidt-Bocking, S. Hagmann, C. L. Cocke, M. Unverzagt, S. Lencinas, and V. Mergel, Phys. Rev. Lett. **71**, 1697 (1993).
[8] H. K. Haugen, L. H. Andersen, P. Hvelplund, and P. H. Knudsen, Phys. Rev. A **26**, 1950 (1982); **26**, 1962 (1982).
[9] H. Knudsen, L. H. Andersen, P. Hvelplund, G. Astner, H. Cederquist, H. Danared, L. Liljeby, and K.-G. Rensfelt, J. Phys. B **17**, 3545 (1984).
[10] L. H. Andersen, P. Hvelplund, H. Knudsen, S. P. Møller, J. O. P. Pedersen, S. Tang-Petersen, E. Uggerhøj, K. Elsener, and E. Morenzoni, Phys. Rev. A **41**, 6536 (1990).
[11] H. Knudsen, Hyperfine Interact. **109**, 133 (1997).
[12] K. Paludan, H. Bluhme, and H. Knudsen, J. Phys. B **30**, 3951 (1997).
[13] H. Knudsen, H.-P. E. Kristiansen, H. D. Thomsen, U. I. Uggerhøj, T. Ichioka, S. P. Møller, C. A. Hunniford, R. W. McCullough, M. Charlton, N. Kuroda, Y. Nagata, H. A. Torii, Y. Yamazaki, H. Imao, H. H. Andersen, and K. Tökési, Phys. Rev. Lett. **101**, 043201 (2008); Nucl. Instrum. Methods Phys. Res. Sect. B **267**, 244 (2009).
[14] J. F. Reading and A. L. Ford, Phys. Rev. Lett. **58**, 543 (1987).
[15] A. L. Ford and J. F. Reading, J. Phys. B **23**, 2567 (1990).
[16] J. F. Reading and A. L. Ford, J. Phys. B **20**, 3747 (1987).
[17] L. A. Wehrman, A. L. Ford, and J. F. Reading, J. Phys. B **29**, 5831 (1996).
[18] L. Nagy, J. H. McGuire, L. Végh, B. Sulik, and N. Stolterfoht, J. Phys. B **30**, 1939 (1997).
[19] M. McCartney, J. Phys. B **30**, L155 (1997).
[20] L. Végh, Phys. Rev. A **37**, 992 (1988).
[21] T. Kirchner, M. Horbatsch, E. Wagnerand, and H. J.Lüdde, J. Phys. B **35**, 925 (2002).
[22] J. X. Shao, X. M. Chen, Z. Y. Liu, R. Qi, and X. R. Zou, Phys. Rev. A **77**, 042711 (2008).
[23] J. X. Shao, X. R. Zou, X. M. Chen, C. L. Zhou, and X. Y. Qiu, Phys. Rev. A **83**, 022710 (2011).

[24] R. D. DuBois, A. C. F. Santos, and S. T. Manson, in *Proceedings of the XXIII Symposium on Ion Atom Collisions, Conference Program* (ISIAC, Beijing, China, 2013), p. 15.

[25] R. D. DuBois, S. T. Manson, and A. C. F. Santos, in *Proceedings of the XXVIII International Conference on Photonic, Electronic and Atomic Collisions, Conference Program*, edited by G. Xiao, X. Cai, D. Ding, X. Ma, and Y. Zhao (ICPEAC, Lanzhou, China, 2013), Abstract We P71.

[26] M. B. Shah and H. B. Gilbody, J. Phys. B **18**, 899 (1985).

[27] M. B. Shah, P. McCallion, and H. B. Gilbody, J. Phys. B **22**, 3037 (1989).

[28] R. D. DuBois, Phys. Rev. A **33**, 1595 (1986).

[29] O. Woitke, P. A. Závodszky, S. M. Ferguson, J. H. Houck, and J. A. Tanis, Phys. Rev. A **57**, 2692 (1998).

[30] O. Heber, B. B. Bandong, G. Sampoll, and R. L. Watson, Phys. Rev. Lett. **64**, 851 (1990).

[31] J. L. Shinpaugh, J. M. Sanders, J. M. Hall, D. H. Lee, H. Schmidt-Bocking, T. N. Tipping, T. J. M. Zouros, and P. Richard, Phys. Rev. A **45**, 2922 (1992).

[32] D. Hennecart, X. Husson, D. Lecler, I. Lesteven-Vaisse, and J. P. Grandin, Radiat. Effects Defects Solids **110**, 141 (1989).

[33] H. Berg, J. Ullrich, E. Bernstein, M. Unverzagt, L. Spielberger, J. Euler, D. Schardt, O. Jagutzki, H. Schmidt-Bocking, R. Mann, P. H. Mokler, S. Hagmann, and P. D. Fainstein, J. Phys. B **25**, 3655 (1992).

[34] H. Berg, O. Jagutzki, R. Dörner, R. D. DuBois, C. Kelbch, H. Schmidt-Bocking, J. Ullrich, J. A. Tanis, A. S. Schlachter, L. Blumenfeld, B. d'Etat, S. Hagmann, A. Gonzales, and T. Quinteros, Phys. Rev. A **46**, 5539 (1992).

[35] R. D. DuBois, L. H. Toburen, and M. E. Rudd, Phys. Rev. A **29**, 70 (1984).

[36] V. V. Afrosimov, Yu. A. Mamaev, M. N. Panov, and N. V. Fedorenko, Sov. Phys. Tech. Phys. **14**, 109 (1969).

[37] V. V. Afrosimov, Yu. A. Mamaev, M. N. Panov, and V. Uroshevich, Sov. Phys. Tech. Phys. **12**, 512 (1967).

[38] V. V. Afrosimov, G. A. Leiko, Yu. A. Mamaev, and M. N. Panov, Sov. Phys. JETP **40**, 661 (1975).

[39] A. L. Ford and J. F. Reading, J. Phys. B **21**, L685 (1988).

[40] M. E. Rudd *et al.*, Rev. Mod. Phys. **64**, 441 (1992).

[41] T. Schneider, P. L. Chocian, and J.-M. Rost, Phys. Rev. Lett. **89**, 073002 (2002).

[42] M. E. Rudd, R. D. DuBois, L. H. Toburen, C. A. Ratcliffe, and T. V. Goffe, Phys. Rev. A **28**, 3244 (1983).

[43] E. C. Montenegro, G. M. Sigaud, and R. D. DuBois, Phys. Rev. A **87**, 012706 (2013).

[44] E. C. Montenegro, A. C. F. Santos, and G. M. Sigaud, in *The CAARI 2000: Sixteenth International Conference on the Application of Accelerators in Research and Industry*, edited by I. L. Morgan, J. L. Duggan, and M. Hall, AIP Conf. Proc. No. 576 (AIP, Melville, 2001), p. 96.

[45] A. Müller, W. Groh, U. Kneissl, R. Heil, H. Ströher, and E. Salzborn, J. Phys. B **16**, 2039 (1983).